Micro and Nano Systems Letters

LETTER

Open Access

Quasi-statically actuated MEMS scanner with concentric vertical comb electrodes

Daehwan Chae[1], Do-hyeon Jeong[1], Seong-jong Yun[1], Kyoung-woo Jo[1] and Jong-Hyun Lee[1,2*]

Abstract

A quasi-static (QS) MEMS mirror scanner with concentric vertical combs (CVC) is presented. The increase rate of overlapped area of the CVC, tends to show larger values and more uniform than that of conventional vertical combs, resulting in improved linearity and scanning angle, respectively. In this paper, the performance of the QS scanner with CVC, whose equivalent mirror diameter is 3.9 mm, was theoretically analyzed and compared with the fabricated one and also other types of vertical combs such as staggered vertical combs (SVC) and angular vertical combs (AVC). The linearity was less than 0.1%, and the average value of the experimental OSA (optical scanning angle) was up to 13.5 degrees, which is only 1/3 and 39% larger than other scanners, respectively, under the condition that the configuration and dimension of each MEMS scanner is similar each other.

Keywords MEMS scanner, Concentric vertical comb, Angular vertical comb, Quasi-static drive, Linkage mechanism

Introduction

MEMS scanner is reflecting mirror with rotational movement fabricated by Si-based semiconductor manufacturing process. MEMS scanners offer the advantages of compact size leading to rapid operation, and low power consumption. Consequently, they find practical applications in fields that demand miniaturization, such as AR display, LiDAR and medical imaging. While MEMS scanners come with various driving mechanisms, such as electrostatic, piezoelectric, electromagnetic, electrothemal etc., among them, the electrostatic comb-drive method stands out for its near absence of hysteresis and relative ease of fabrication [1–5].

The comb-drive actuator refers to a structure in which two sets of thin vertical electrodes are stacked in a lateral direction in the form of interdigitated electrodes, namely the stator and the rotor. When these parallel electrodes are arranged, they form capacitance. Upon applying a voltage between the two interdigitated electrodes, one electrode accumulates a positive charge (+Q) while the opposite electrode accumulates a negative charge (−Q). According to Coulomb's law, these charges (accumulation) generates an attractive force in the direction where the capacitance is maximized, i.e., the direction with maximized overlapped area [6].

By inducing rotational degrees of freedom in the actuator's spring, it becomes possible to enable angular movement since rotation increases the overlapped area of combs. In this paper, our objective is to improve linearity and enlarge scanning angle of a micro mirror scanner that is driven by the electrostatic comb-drive actuator.

Theoretical analysis of comb actuators

The resonance (RS) type scanner is a method that utilizes the natural resonant frequency determined by the characteristics of the mirror and the spring featuring a large scanning angle [7]. The RS type scanner has the advantage of having a rigid spring and can be easily fabricated as it does not require a height difference between the fixed coms (stator) and movable combs (rotor). However, it has the limitation of being able to

*Correspondence:
Jong-Hyun Lee
jonghyun@wemems.co.kr
[1] WeMEMS R&D Center, 67 Saebitgongwon-Ro, Gwangmyeong-Si, Gyeonggi-Do 14348, Korea
[2] Gwangju Institute of Science and Technology, 123 Cheomdangwagi-Ro, Buk-Gu, Gwangju 61005, Korea

control the operating frequency only within a narrow range in a sinusoidal waveform.

On the other hand, the quasi-static (QS) type scanner has the advantage of being capable of driving the mirror with frequencies and waveforms desired by the user, when driving frequency is sufficiently smaller than resonant frequency. However, to achieve this, it requires an initial offset in height or angular displacement between the fixed and movable combs, unlike the resonance type, making its fabrication more complicated [8].

Figure 1 shows an example of a comb-drive actuator. When a voltage difference occurs between the fixed and movable comb electrodes, the rotor rotates by an angle $d\theta$, causing the cross-sectional area A between the two electrodes to increase by dA. The torque T obtained by the actuator is proportional to V^2 and $\delta A/\delta\theta$, as indicated in Eqs. (1, 2).

$$E_C = -\frac{1}{2}CV^2 = -\frac{1}{2}\frac{\varepsilon A}{g}V^2 \tag{1}$$

$$T = \frac{\delta E_c}{\delta\theta} = -\frac{1}{2}\frac{\varepsilon}{g}\frac{\delta A}{\delta\theta}V^2 \tag{2}$$

where, E_C = energy stored in comb electrodes, C = capacitance, V = input voltage, T = torque, ε = permittivity, A = cross-section area and g = gap between combs.

Here, when $\delta A/\delta\theta$ maintains as a constant value, the torque T shows linear behavior, proportional to V^2. In reality, $\delta A/\delta\theta$ is not a constant value and tends to slightly vary depending on the comb's shape and angular position. Moreover, the limit of rotational angle, where $\delta A/\delta\theta$ is kept close to a constant value, depends on the structure of the comb drive such as comb length, initial offset in height, and thickness of device layer, i.e. on the types of comb configuration.

Up to now, the conventional electrostatic actuators of the QS scanners have been configured in the form of SVC (staggered vertical combs) or AVC (angular vertical comb), as shown in Fig. 2a, b [9–12]. The fabrication of the SVC requires twice DRIE (Deep Reactive Ion Etching) of a silicon-on-insulator (SOI) wafer. Therefore, these structures increase the complexity in the device fabrication leading to high cost. Furthermore, SVC is accompanied by the problem that the driving angles of the rotor is comparatively small [13, 14].

Meanwhile, AVC (angular vertical comb) type can be manufactured with a simple semiconductor process. For instance, AVC type scanner only needs single DRIE process to form comb drive. However, its linearity is poor due to non-uniform increments of $\delta A/\delta\theta$ as shown in Fig. 3b and Table 1. In the calculation for three types of MEMS scanner, the thickness of device layer, the length of movable comb and overlapped

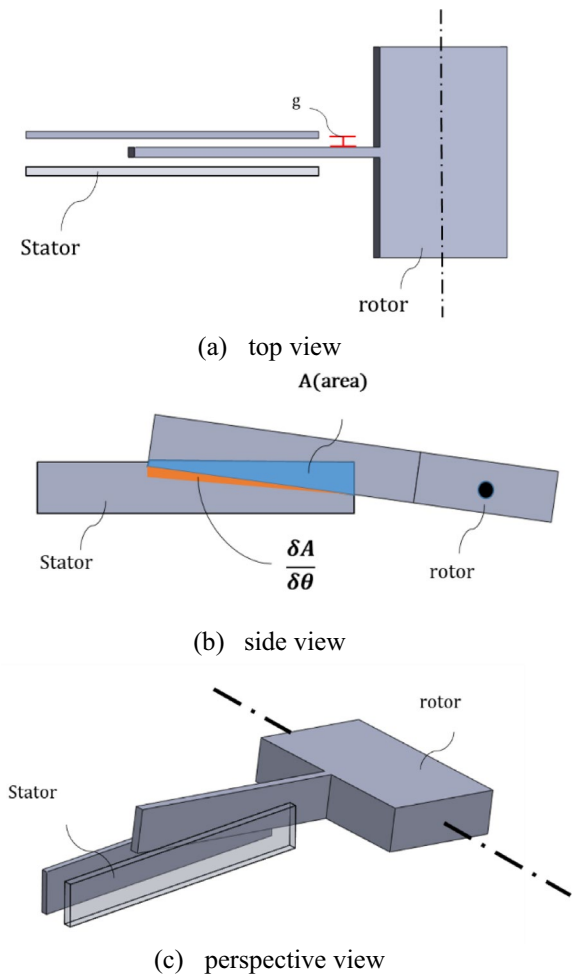

Fig. 1 Comb-driven rotation actuator: (**a**) top view, (**b**) side view, and (**c**) perspective view

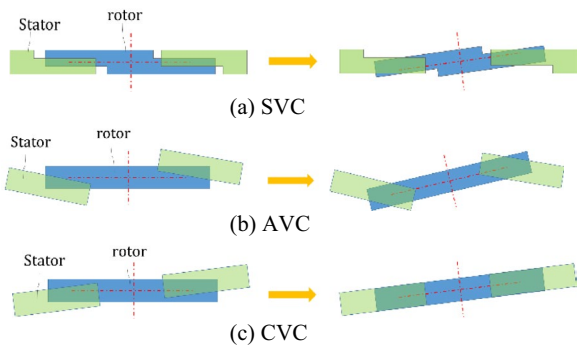

Fig. 2 Driving mechanism of (**a**) SVC (staggered vertical comb), (**b**) AVC (angular vertical comb) and (**c**) CVC (concentric vertical comb)

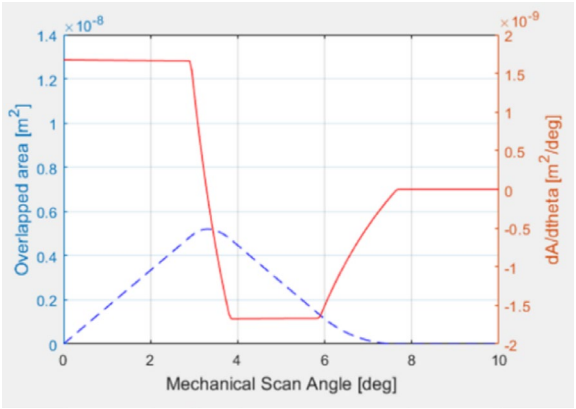

(a) SVC

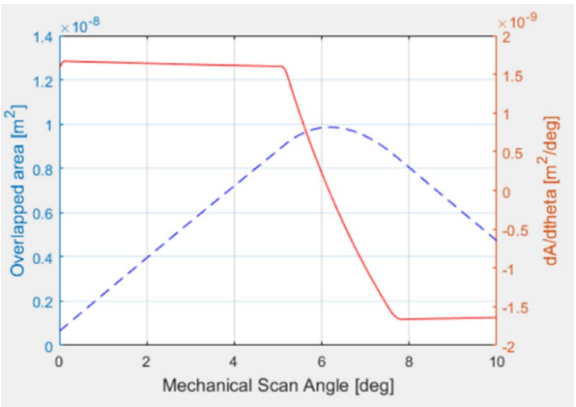

(b) AVC

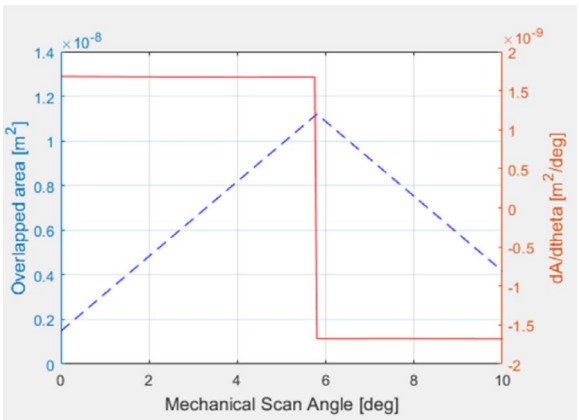

(c) CVC

Fig. 3 *A* (area) and $\delta A/\delta\theta$ varying with mechanical angle of (**a**) SVC (staggered vertical comb), (**b**) AVC (angular vertical comb), and (**c**) CVC (concentric vertical comb), Dotted line overlapped area (*A*), Solid line $\delta A/\delta\theta$

Table 1 Linearity comparison of quasi-static MEMS scanners

Comb type	SVC	AVC	CVC
Mechanical angle [deg]	2.9	5.1	5.8
Linearity [%/deg]	0.288	0.795	0.083

length of movable comb and fixed comb are 70 μm, 180 μm, and 160 μm, respectively.

To enhance a linearity of scanning angle with the square of input voltage (V^2), we propose to use CVC type MEMS scanner. CVCs are different from AVC in that the movable combs are always angularly aligned with the stationary comb regardless of angular position of the movable electrodes. Thus, the increments of the overlapping area in the CVC type is almost constant, resulting in an improvement in linearity. Furthermore, CVC structure maximizes overlapped area of comb thereby increasing the maximum rotation angle.

MEMS design

The proposed CVC structure was incorporated into a Si-based quasi-static (QS) MEMS mirror scanner fabricated using silicon-on-insulator (SOI) wafers. There have been attempts to implement CVC (in other words, aligned AVC). CVC structure for a MEMS mirror using reflow was proposed, but was not actually fabricated [15]. Another approach aimed to achieve a CVC structure by inducing permanent deformation in silicon at high temperature, around 900 ℃ [16], but might damage the reflective surface in case of aluminum coating.

The CVC structure in this paper can take advantages of a simple three-layer microfabrication process similar to the conventional AVC fabrication, even though it requires an microassembly of tiling the part of comb electrodes [17].

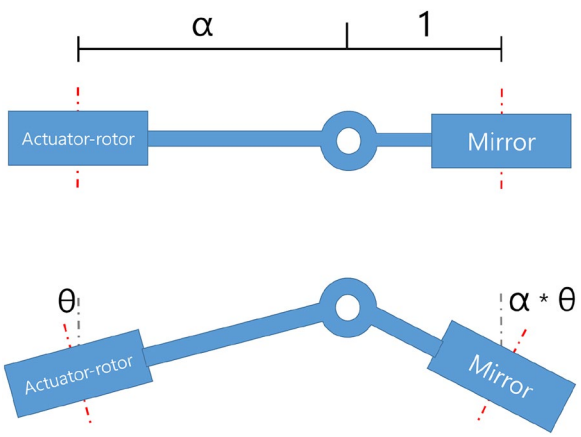

Fig. 4 Angle amplifying linkage mechanism

Angle-amplifying linkages, as shown in Fig. 4, are also employed to magnify the scanning angle. In the design, these linkages provide a magnification ratio of $\alpha = 2$. While the theoretical maximum rotation angle of the actuator under simulation conditions is 11.6 degrees (OSA), this linkage system enables the mirror to achieve even greater rotation.

The rotor of the comb driven MEMS scanner is designed to rotate in a torsional mode. The stator (stationary combs) is tilted and fixed at a certain angle, enabling the movable combs to rotate about the same axis of the rotor, as shown in Fig. 5. To lower the driving voltage, the comb electrodes is placed as many as possible by connecting the linkage between the mirror and actuator.

The experimental driving characteristics of the CVC scanner will be compared with the theoretical one, and also with the formerly manufactured AVC scanners. Those two chips have identical chip size and the mirror size (ellipsoidal) as shown in Fig. 6 and the 1st mode (rotation mode) frequencies are similar each other. Note that scanners with AVC and CVC actuators were manufactured and their performances are compared, whereas those with SVC actuators were theoretically evaluated.

In the simulation, an input voltage of 130 V is applied to the scanner, resulting in an OSA of 15.47 degrees. This outcome is achieved by deliberately lowering the spring stiffness to increase the rotation angle, consequently yielding a slightly low resonance frequency of 371 Hz for the mirror's first mode.

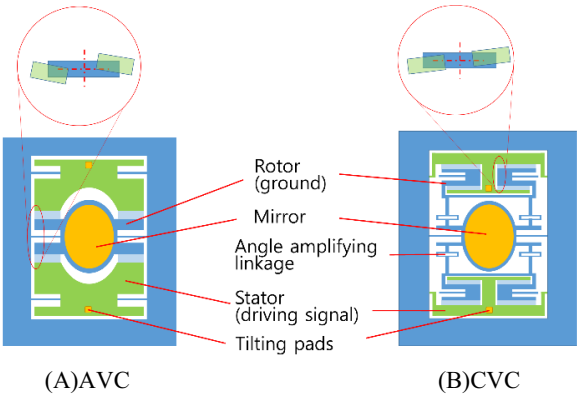

Fig. 6 Top view schematics of the scanner chips with (**a**) AVC (angular vertical comb) and (**b**) CVC (concentric vertical comb)

Experiments

The proposed scanner chips were fabricated through a simple process using three masks, as depicted in Fig. 7.

The overall structure and morphology of the produced chip are displayed in the photo image of Fig. 8, where the rotation axes of the stator and rotor coincide, along with a link structure to amplify the OSA of the mirror.

The actuator section of the chip exhibits an initial angle in the SEM image of Fig. 9 through the tilting process, as

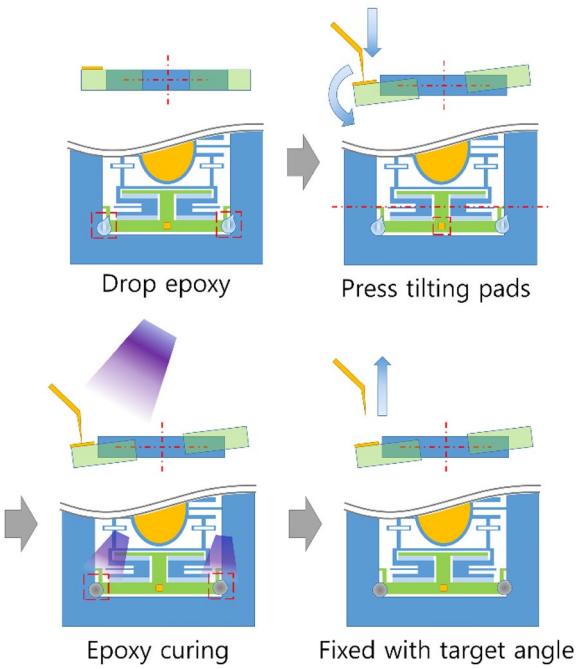

Fig. 5 Design of process sequence for tilting the fixed comb electrodes

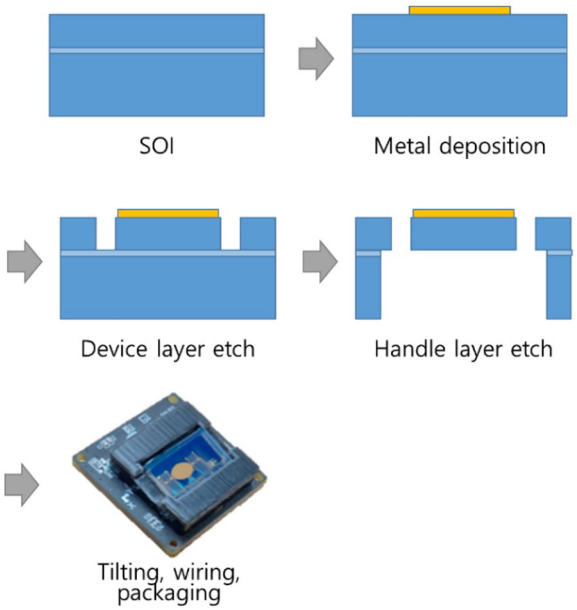

Fig. 7 Fabrication process of the packaged MEMS scanning mirror

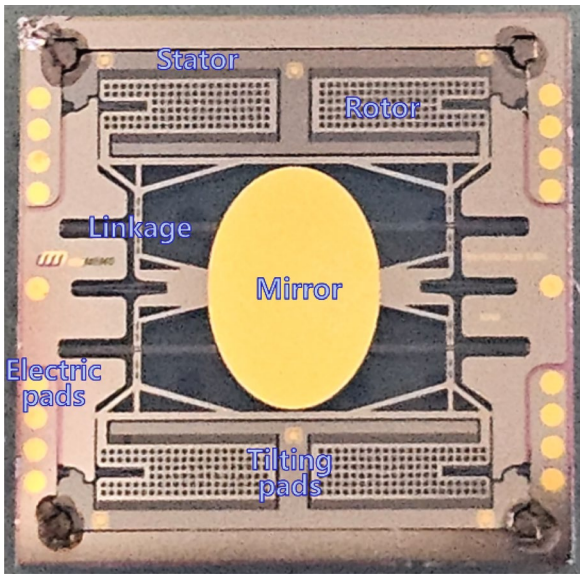

Fig. 8 Photo image of the fabricated scanner chip

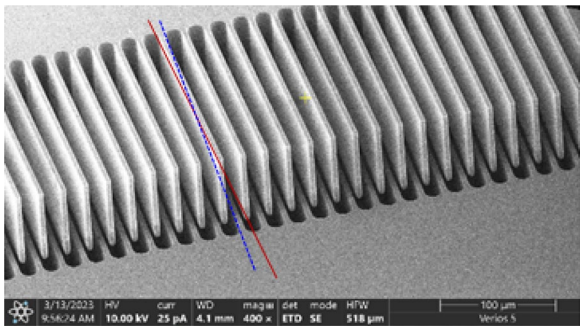

Fig. 9 SEM image of the concentric vertical combs (CVC) actuator

depicted in Fig. 9. The extension lines of the lower comb (represented by a blue dashed line) and the upper comb (represented by a red solid line) are not parallel to each other, indicating upper combs are tilted to the lower ones.

The experimental setup is shown in Fig. 10. The packaged MEMS scanner is positioned and fixed on the pedestal while electrically interfaced to the connector. Upon receiving the driving signal, the Au-coated mirror at the central part of the chip rotates about the torsional springs. The reflected light reaches the position sensitive detector (PSD), generating electrical signals correlated with the OSA.

Figure 11 shows the DC driving characteristic of the fabricated quasi-static MEMS scanner with CVC. The curves in blue and orange represent experimental and theoretical OSA, respectively. The theoretical value is very close to the experimental value, indicating high linearity with respect to the V^2. This implies that the area

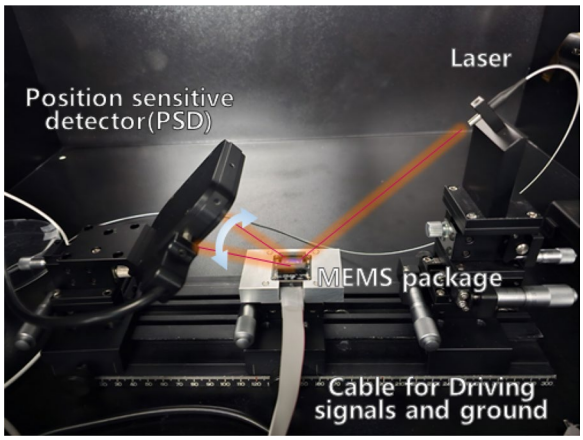

Fig. 10 experimental setup

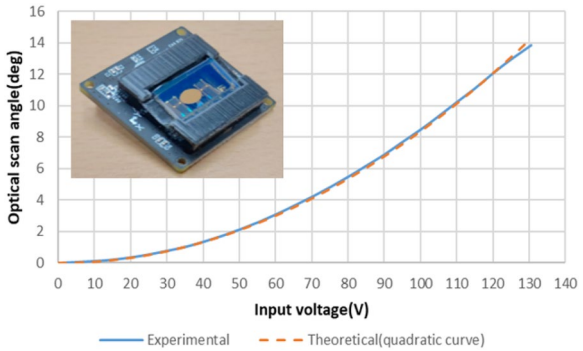

Fig. 11 Static response curve (V_{dc}–OSA) of the quasi-static MEMS scanner with CVC electrodes

Table 2 Comparison of optical scanning angle (OSA) for quasi-static MEMS scanners

Comb type	AVC	CVC
Mean ± σ	9.7 ± 0.6	13.5 ± 1.2
Σ [%]	6.2	8.9

change rate of the combs is consistently maintained constant, resolving the nonlinearity caused by drastic decreases in capacitance at the end of the rotation angle, so-called C-nonlinearity [18].

The high linearity observed between V^2 and the mirror rotation angle suggests greater convenience in generating scanning outputs in a triangular waveform. In the near future, we plan to introduce a new MEMS scanner driven with a high linearity between input voltage (V) and rotation angle of a mirror. The CVC actuator with this high linearity will be beneficial to generate arbitrary motion in the MEMS scanners.

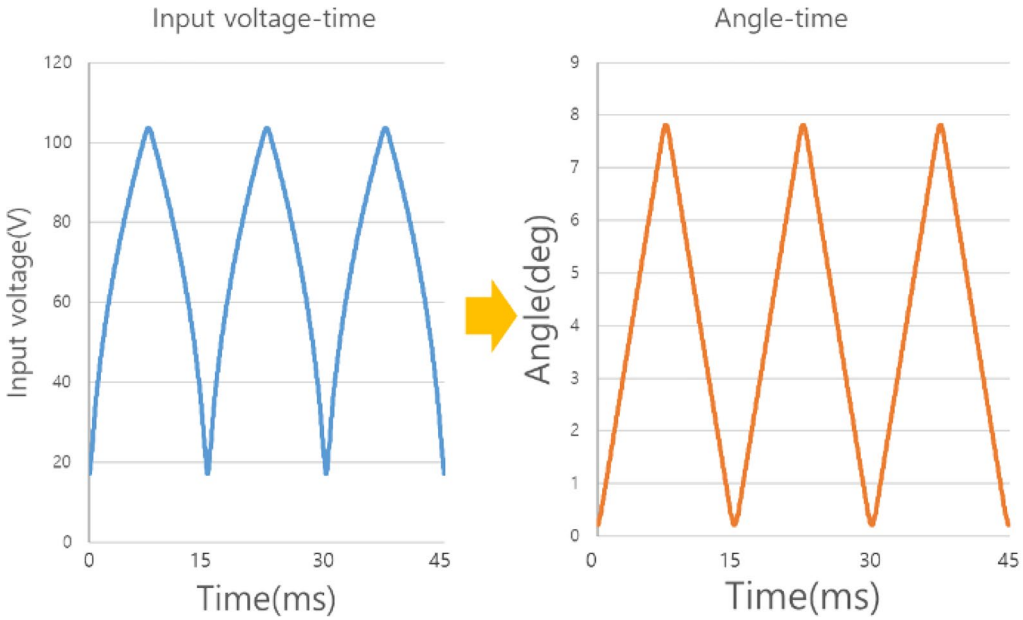

Fig. 12 Theoretical input shaping process of the generation of input drive voltage for targeted scanning output waveform

In Table 2, the maximum OSA of the scanner is up to 15°, and average OSA (13.5 degrees) is increased by 39% compared to other types of MEMS scanners. The enlarged angular movement of the MEMS scanner is partially due to the linkage system, allowing it to surpass the theoretical maximum rotating angle estimated considering only comb configuration.

The 1st mode frequency of rotational mirror motion is 343 Hz, and its deviation from the theoretical one is negligibly small. When it comes to the 1st mode frequency, they show similar characteristic regardless of the type of the MEMS scanner.

Input shaping

QS-type scanners are in high demand due to their capability to operate with triangular waveforms, which is desirable in the most of the scanner applications. Actually, there are various waveforms requested, including saw tooth, square waves, and even arbitrary waveforms.

Theoretically, an arbitrary waveform in angular scanning can be generated by using a certain input voltage whose shape corresponds to the targeted waveform of the output scanning, as shown in Fig. 12. This theory works well for sinusoidal waveform output, which has only one frequency component, whereas it does not work for complex waveforms such as triangular waves, resulting in the occurrence of ripples in the output waveform.

In case of complex input signals, such as triangular or rectangular waveform, they have high order terms in the frequency domain. When one of the high order frequencies are close to the resonant frequency of the system, this might be a main cause of the ripple in the motion of the MEMS mirror.

By applying an input shaping method based on the transfer function and static response of the MEMS mirror scanner, the shaped input waveform was theoretically calculated for the target output of triangular output waveform [18]. When the shaped input was applied to the scanner, the triangular output was obtainable as shown in Fig. 13. The ripples can be further suppressed by employing low pass filter at the cost of reducing the usable range in optical scan angle.

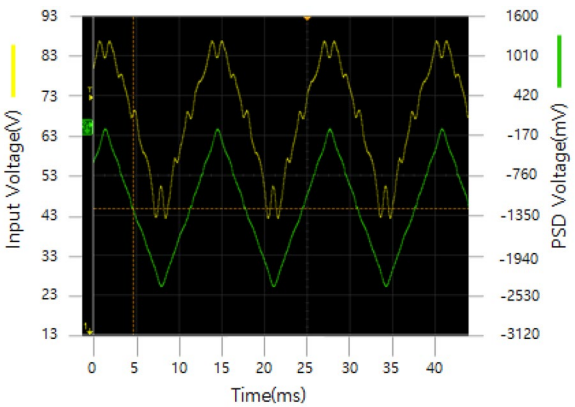

Fig. 13 Waveform generated by applying input shaping method, shaped input drive voltage, output voltage of PSD correlated with optical scanning angle)

Conclusions

It was confirmed that linearity and the scanning range were improved compared to the SVC and AVC MEMS scanners. Input voltage in certain waveforms such as triangular wave, can induces irregular angular output with a serious level of ripples caused by resonance mode of the scanner. To achieve desired output, it is recommended to apply the shaped input acquired from transfer function and static response curve of the scanner.

Increasing the stiffness of the torsional spring, which would increase the resonant frequency, can be an option to decrease ripple but it will reduce maximum rotation angle of mirror. In the near future, we will report on the improved QS MEMS scanner whose static response is linearly proportional to the input voltage by adopting multiple level of comb electrodes.

Acknowledgements
Not applicable.

Author contributions
Experiment design and conceptualization: DC and JL. Chip design: DC. Chip packaging: SY. Methodology and data analysis: DC and DJ. Supervision: KJ and JL. Wrighting and editing of the manuscript: DC and JL.

Funding
This work was partially supported by the WeMEMS research project funded by the Technology Development Program of MSS (S3039876) and by the GIST Research Project grant(k16460) funded by the GIST in 2023.

Availability of data and materials
All data generated or analyzed during this study are included in this published article.

Declarations

Ethics approval and consent to participate
Not applicable.

Consent for publication
Authors consent the SpringerOpen license agreement to publish the article.

Competing interests
The authors declare that they have no competing interests.

Received: 26 September 2023 Accepted: 28 November 2023
Published online: 31 January 2024

References

1. Xu XH et al (2007) Design, fabrication and characterization of a bulk-PZT-actuated MEMS deformable mirro. J Micromech Microeng 17(12):2439
2. Baran U et al (2012) Resonant PZT MEMS scanner for high-resolution displays. J Microelectromechan Syst 21(6):1303–1310
3. Bernstein J et al., (2003) Two axis-of-rotation mirror array using electromagnetic MEMS, the sixteenth annual international conference on micro electro mechanical systems, Kyoto, Japan
4. Dong R et al (2018) Mirror angle tuning of electromagnetic micro-mirrors with oscillation compensation. IEEE Transact Syst Man Cybernet Syst. 50(8):2969–2977
5. Hu F et al (2010) A MEMS micromirror driven by electrostatic force. J Electro 68(3):237–242
6. Morkvėnaitė-Vilkončienė I et al (2022) Development of electrostatic microactuators: 5-year progress in modeling, design, and applications. Micromachines. 13(8):1256
7. Lee M et al (2022) Capacitive sensing for 2-D electrostatic MEMS. IEEE Sens J 22(24):24493–24503
8. Jeong D et al. (2022) Nonlinear characteristics of electrostatic resonant MEMS scanner for AR display, The 3rd MNS Conference, Gwangju, Korea
9. Liu Y et al (2013) Large size MEMS scanning mirror with vertical comb drive for tunable optical filter. Optics Lasers Engineer. 51(1):54–60
10. Schroedter R et al (2019) Silicone oil damping for quasi-static micro scanners with electrostatic staggered vertical comb drives. IFAC-PapersOnLine 52(15):37–42
11. Moon S et al. (2015) An electrostatic two-axis gimbaled mirror scanner with tilted stationary vertical combs fabricated by self-aligned microassembly, International Conference on Optical MEMS and Nanophotonics, Jerusalem, Israel
12. Pamela RP et al. (2002) A scanning micromirror with angular comb drive actuation, Technical Digest. MEMS 2002 IEEE International Conference. Fifteenth IEEE International Conference on Micro Electro Mechanical Systems, Las Vegas, NV, USA
13. Milanović V et al. (2017) Novel packaging approaches for increased robustness and overall performance of gimbal-less MEMS mirrors, SPIE Conference on MOEMS and Miniaturized Systems XVI, San Francisco, CA
14. Zhang W et al (2018) InGaN/GaN micro mirror with electrostatic comb drive actuation integrated on a patterned silicon-on-insulator wafer. Opt Express V26:I6
15. Hah D et al (2004) Theory and experiments of angular vertical combdrive actuators for scanning micromirrors. IEEE J Select Topi Quant Electron 10(3):505–513
16. Kim J et al. (2005) 2-D scanning mirror using plastically deformed angular vertical comb drive actuator, The 13th International Conference on Solid-State Sensors, Actuators and Microsystems, 2005. Digest of Technical Papers. TRANSDUCERS '05., Vol 2
17. Moon S et al (2016) Two-axis electrostatic gimbaled mirror scanner with self-aligned tilted stationary combs. IEEE Photon Technol Lett 28(5):557–560
18. Kim K et al (2019) Input-shaping method based on the experimental transfer function for an electrostatic microscanner in a quasistatic mode. Micromachine 10(4):217

Publisher's Note